Presented at the 4th World Conference on Photovoltaic Energy Conversion, WCPEC-4, June 14 2018, Waikoloa Village, Hawaii USA

Compressive Stress Strategies for Reduction of Cracked Cell Related Degradation Rates in New Solar Panels and Power Recovery in Damaged Solar Panels

Andrew M. Gabor[1], Jason Lincoln[2], Eric J. Schneller[2], Hubert Seigneur[2], Rob Janoch[1], Andrew Anselmo[1], Duncan W. J. Harwood[3], Michael W. Rowell[3]

[1]BrightSpot Automation LLC, Westford, MA, USA

[2]Florida Solar Energy Center, University of Central Florida, Cocoa FL, USA

[3]D2Solar, San Jose, CA, USA

***Abstract* — Some crystalline silicon PV system underperformance is due to the presence of cracked solar cells, and this represents a financial risk for both already installed and future systems. This work describes compressive stress strategies and rear side pressure strategies that can be employed in new panel construction to prevent crack formation as front side mechanical loads from handling, wind, and snow are applied during shipping, installation and in the field. These strategies can also slow the opening of cracks and the related power loss for any cracks that do form. Furthermore, we present concepts for the retrofitting of older installed systems to close already open cracks and regain lost power, or to slow the future degradation of systems with panels that are sensitive to cracked cells.**

Index Terms — cracks, mechanical load testing, photovoltaic modules, reliability, silicon.

I. Introduction

The most common solar panel design, utilizing a front glass coversheet and a polymer backsheet with copper interconnect wires between silicon cells, is sensitive to the tensile stress related cracking of the cells when front side mechanical loads are applied to the panel through handling, snow load, or wind load. These cracks are often closed initially after formation with minimal power loss, but over time the cracks can open up such that metallization is discontinuous across the cracks, leading to higher than desired degradation rates and risks of hot spot heating. Several trends within the industry are helping to reduce the occurrence of such cracks, for example by using glass backsheets to place the cells in the neutral plane mechanically so that cells are not placed into tensile stress under load, or by adopting interconnect methods using electrically conductive adhesives to eliminate solder induced damage in the silicon, such as in shingled panels. Should cracks occur, the trend of using a higher number of interconnect wires on each cell reduces the potential power losses. Still other trends are adding to crack related risks such as reduced frame mass that allows panels to bend more with applied loads, larger panels with higher deflections, thicker interconnect wires to carry the steadily increasing amounts of cell current which then cause more soldering induced microcracks in the silicon [1] , more cell breakage with insufficient encapsulant thickness after low-temperature exposure and panel bending [2-4], and half-cut cells or even narrower shingled cells which have weak laser-cut edges from which cracks are more likely to propagate. In addition, a large installed base of panels exist which are more sensitive to cells cracking with only 2 or 3 busbars, and which already have a high density of cells cracks or which are sensitive to their formation in the future.

Looking forward, the industry could benefit from more choices in improved panels designs and manufacturing methods where either the cells are less likely to crack in the first place, or if they do, the cracks are less likely to contribute to power loss. The industry could also benefit from methods to extend the lifetime of the already installed base of panels sensitive to crack related degradation.

BrightSpot Automation's mechanical load tester, the *LoadSpot*, was designed to allow insight into crack formation, crack opening, and power degradation by leaving the front side open for electroluminescence (EL) and IV measurement. We and others have published results on how closed cracks can open up as front side loads are applied with vacuum behind the panels and the cells are placed into tensile stress [5-8]. As cracks open up, dark inactive areas appear in the EL images and the panel power decreases. We also noticed, but did not previously publish, that the reverse is true, and that by applying rear side loads with air pressure, that already open cracks can be closed with corresponding improvements in the EL image and panel power. An example of such crack closure is shown in Fig. 1 where a rear side load of 1900 Pa results in a remarkable improvement in the EL image of a badly damaged panel that had seen a front load of 5400 Pa and environmental chamber exposure. To our knowledge, this is the first time such crack closure has been documented.

In this work, we explore other more practical methods of placing cells into compressive stress to either make cells less likely to enter high tensile stress regimes as front side loads are applied, or to keep cracks closed should they form. One feature seen in an increasing number of panels is an aluminum cross

bar spanning the width on the rear side of panel and connected to the extruded Al frame on each side. This stiffens the panel and effectively reduces the deflection (and thus tensile stress) vs load. An image of Kyocera panel from 2010 with 2 cross bars is shown below (see Fig. 2). Some of these panels even had a pave in the middle that lightly touches the backsheet or has a narrow air gap, and such a pad can further reduce panel deflection vs load. In this work, we expand beyond such a crossbar design, and instead allow rear side brace designs that actively apply pressure to the rear side to establish compressive stresses in the cells. We refer to this as the **C**ompression **U**nder **R**ear **L**oad (CURL) approach. We also explore other methods of building in compressive stresses in the lamination and cooling stages. We refer to this as the **L**amination **I**nduced **P**rotective **S**tress (LIPS) approach.

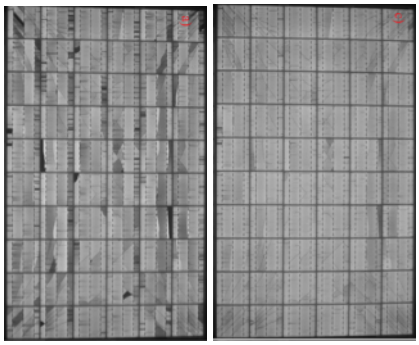

Fig. 1. EL images as a function of applied pressure on the *LoadSpot* load tester: left) No pressure; right) 1900 Pa back side pressure showing crack closure.

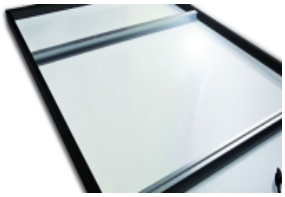

Fig. 2. A Kyocera panel with 2 cross bars.

II. Finite Element Analysis of Compressive Stresses

We used the FEA program Abaqus to model the cell stresses vs applied loads. Fig. 3a shows a simulation of cell deflection and stress from the application of rear-side air pressure as was the case in the physical experiment shown in Figure 1. In comparison, Fig. 3b shows corresponding maps to a scenario with the same peak deflection but where the pressure was applied with a rear-side brace spanning the width of the panel connected to a 10cm x 3.5cm pressure pad in the center of the panel. The pad is modeled here as applying constant pressure to the backsheet even as front pressure is applied. In comparing these two sets of maps we see that the brace approach places over 50% of the cells into compressive stress, but concentrates more deflection and compressive stress in the center region of the panel than does the air-pressure approach. We also note that the FEA model accurately predicts panel deflection in the center region of panel as compared to caliper measurements, but we see deflections along the short axis of the frame that are not being accurately predicted by the model.

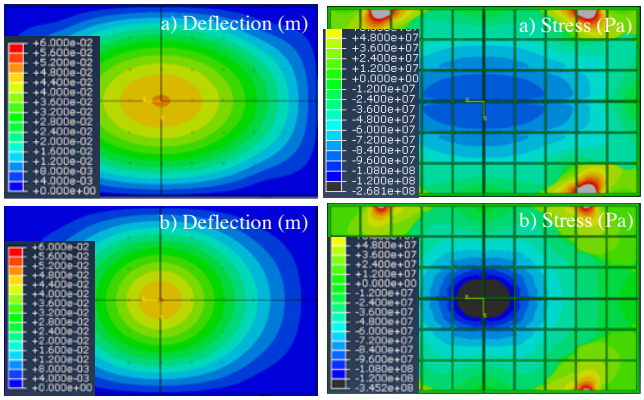

Fig. 3. Simulated maps of panel deflection and cell stress for a) full rear-side air pressure of +2000 Pa, and b) application of pressure from a brace pad at the center of the panel yielding the same peak deflection.

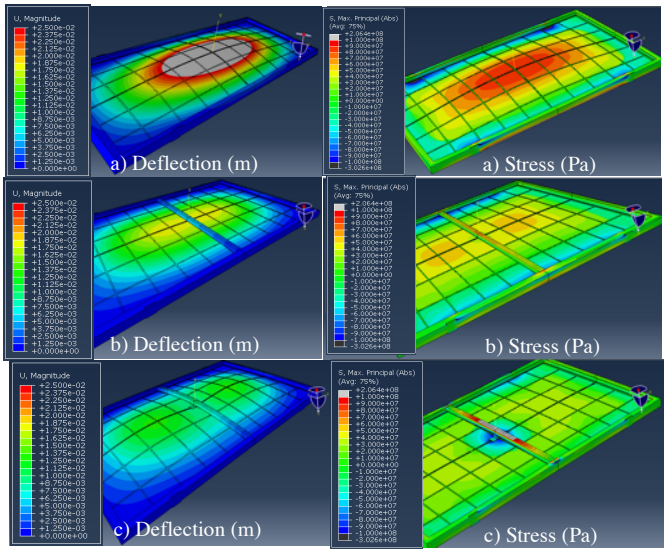

Fig. 4. Simulated maps of panel deflection and cell stress for a front side load of -2400 Pa applied to panels with a) no brace and a standard frame, b) a brace and a reduced mass frame but no pressure pad, and c) a brace and a reduced mass frame and a pressure pad that pressed on the backsheet to deflect the glass surface by 1 cm at the 0 Pa state.

Fig. 4a shows maps for the scenario where a front side load of -2400 Pa is applied with no brace, thus placing the cells into tensile stress. Fig. 4b shows around a 50% reduction in cell stress by when this same load is applied to a panel with a brace weight of 0.48 kg and a frame with reduced wall thickness to fully compensate for this added weight. In this case there was no pressure pad pressed against the backsheet, but the front side load caused the backsheet to touch the brace in the middle. Fig. 4c is similar to the 4b case, except that here a pressure pad was first pressed against the backsheet to deflect the glass by 1 cm in the 0 Pa state. Here the peak stress was further reduced by

~25%, and a smaller percentage of the cells were placed into tensile stress with some cells still remaining in compression.

III. Crack Closure with Rear Side Braces

We constructed a metal brace with flexible features to allow the application of variable amounts of pressure to an arbitrary number of pads on the panel backsheet, and clamped the brace to the lip of the panel frame at the midpoint of the long edge (see Fig. 5). As we applied pad pressure, we measured the deflection at 7 points across the panel width at the ¼, ½, and ¾ points along the long edges by place a straight edge across the frame and measuring the change in distance to the backsheet with digital calipers. Prior to application of brace pressure, we clamped the panel to a rigid frame of Schedule 40 pipe using Ironridge rails, U-bolts, and end-clamps at the 1/5 and 4/5 points along the long edges as is commonly performed in field installations.

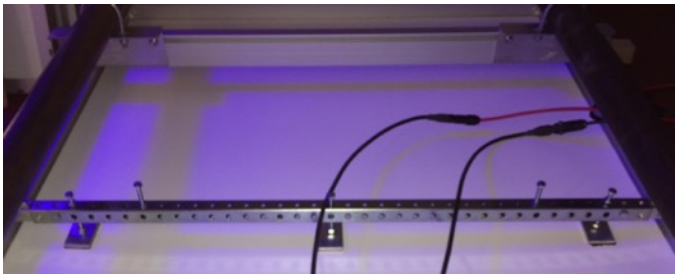

Fig. 5. A brace with 3 pressure pads applied to a panel.

Fig. 6a shows the EL images (forward biased at $-I_{sc}$) of the damaged monocrystalline silicon panel with no pressure applied. Fig. 6b shows the EL image and displacement curves with a single center pressure pad, while Fig. 6c corresponds to the use of 2 pressures pads where the center of each pad was placed 9.5 cm from the inside face of the frame. The use of a single pressure pad yields a displacement profile with a much sharper peak in the center than the use of 2 pads near the edge which yields a much flatter profile in the middle and sharper slopes near the frame. Likewise, the middle pad yields very effective crack closure near the center of the panel and moderate to weak crack closure near the sides, while the edge pads yield much more effective crack closure near the edges, but little if any improvement in the center. We showed that by using all 3 pads simultaneously, we could tailor the profile to achieve different tradeoffs between center and edge crack closure.

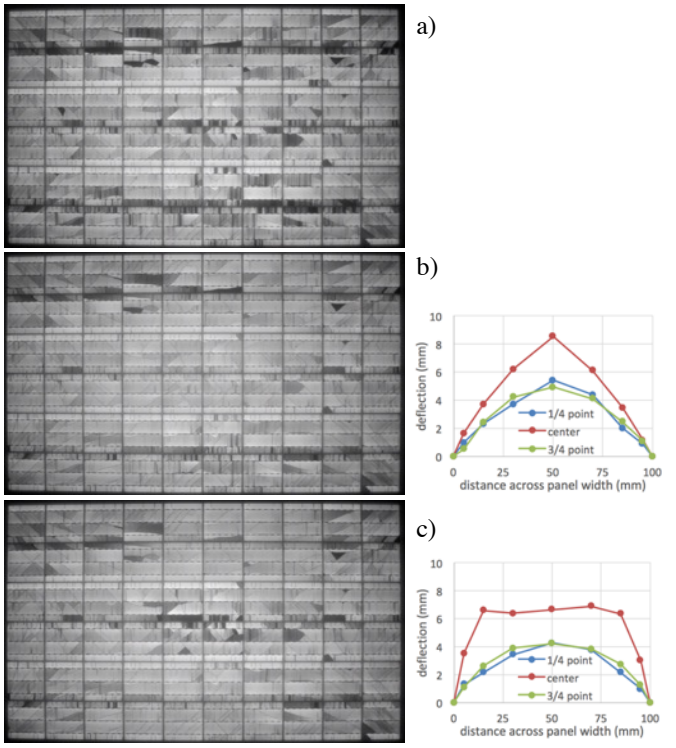

Fig. 6. EL images and deflection maps across the panel width at a) no pressure, b) a brace with a center pressure pad, c) 2 edge pads.

In an experiment with a different badly damaged panel, we applied various front and rear side loads as is shown below. Fig. 7a shows the EL image with no load, while Fig. 7b shows the opening of many closed cracks with a front side load of -2400 Pa using partial vacuum from the rear side on the *LoadSpot*. Conversely, Fig. 7c shows dramatic crack closure of previously open cracks with application of air pressure of +1900 Pa from the back side. We achieved a similar level of crack closure by applying a brace with a center pad displacement of 1 cm at the center (Fig. 7d), and an even higher level of crack closure at a displacement of 1.6 cm (Fig. 7e) which increased the panel power by 4.9W. By first applying a brace with a 1-cm deflection and then mounting the panel on the *LoadSpot* and applying a front side pressure of -2400 Pa, we can see (Fig. 7f) that the crack opening was far reduced in comparison to the equivalent case without the brace. Interestingly, the application of the front side pressure actually caused even more crack closure in the center of the panel than was the case with no *LoadSpot* applied pressure. Application

of 2 or more braces conceivably would further improve the crack closure.

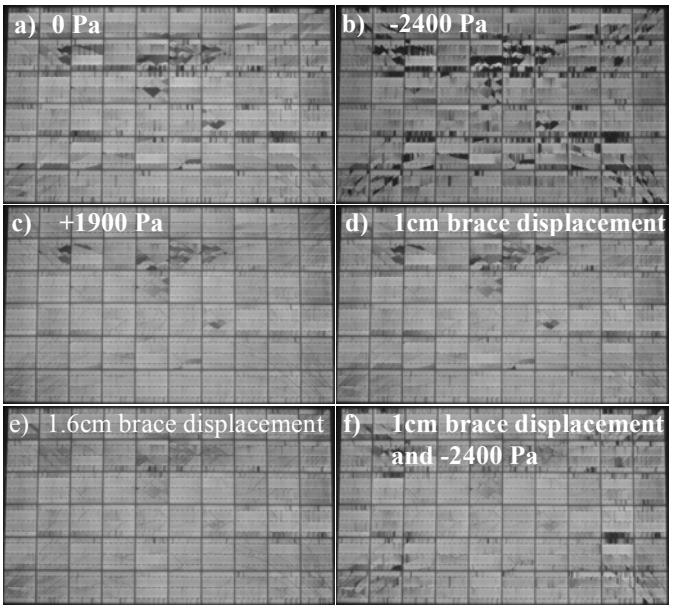

Fig. 7. EL images of a damaged panel at a) 0Pa, b) -2400Pa, c) +1900 Pa, d) Brace applied at 1cm displacement, e) Brace applied 1.6cm displacement, f) Brace applied at 1cm displacement with -2400Pa load.

In addition to improved EL images by application of the brace, we also saw improvements in panel power. The above panel and 2 other badly damaged panels saw power boosts of 4.9 W_p, 9.0 W_p, and 10.3 W_p after application of a brace with approximately 1.6 cm deflection.

IV. Brace Applications and Concerns

A brace could be applied either during the original construction of solar panels in a co-optimized cost-weight-performance design, or it could be performed as a retrofit to pre-existing panels to either prevent future degradation or to improve the power/safety of already damaged panels. A variety of concerns are relevant to implementation of such braces including: 1) component costs, 2) labor costs, 3) panel mass changes, 4) effectiveness of the solution, 5) durability of the solution over time, 6) new problems arising from the brace, 7) aesthetics, and 8) warranty violation.

In terms of the labor cost concern, let us consider a practical example. BrightSpot Automation and its partners offer field testing of panels with its EL camera product, and such testing involves access to the rear side of the panels (see Fig. 8) for disconnecting and re-connecting cables between panels. If a damaged panel is found through the EL inspection, the field worker could easily apply a brace to the panel at the same time that the cables are being reconnected with little additional labor cost. Implementing the CURL solution at such a point in time might immediately improve the performance of the entire string of connected panels, reduce the risks associated with hot spot heating, and serve as a temporary fix or permanent fix (particularly if equivalent replacement panels are unavailable) to the system. BrightSpot is designing a brace product (*BrightBrace*) and tooling to install the brace in a way that this operation can occur in minimal time by one worker without removal of the panel from the rack. While applying a brace to an undamaged panel raises warranty violation concerns, applying a brace to an already compromised panel may meet with less resistance.

Fig. 8. Reconnecting cables between panels after a field EL test. A brace field retrofit could occur at the same time.

In terms of panel mass in new construction, it may be challenging to implement a solution that increases the total mass of the product as this influences the ease of installation and shipping costs. Panel mass also generally correlates to cost, so we would like a solution that does not increase panel mass, and if possible, enables a reduction. In Table I below, we show the typical mass of the glass and frame in a 60-cell panel. We also show examples of proposed change to the panel construction and how they compare. The addition of a brace to new panel construction may add say 0.7 kg, but the improved performance due to the brace may allow mass to be removed from the rest of the frame or from the glass to partially, fully, or more than fully offset the brace mass while still maintaining superior characteristics of cell stress vs applied load. Such savings in mass may help enable the implementation of thicker front encapsulant to reduce sensitivity to cell cracking as we describe elsewhere [2-3].

Optically, a panel that is pressed outward from the center by a brace will have a different appearance particularly when viewed at certain angles relative to the sun, and the aesthetics associated with such variation may be undesired in certain types of installations.

While we have shown effective closure of cracks with the brace and P_{max} improvements in excess of 10W, we have not yet demonstrated that these improvements are long-lasting and free of problems in typical field conditions. For example, creep in the encapsulant and other materials from the applied stresses could reduce the applied compressive stress over time, thus allowing cracks to re-open. Additionally, the applied forces could cause undesired effects such as a failure related to the frame, deterioration of the backsheet under the pads, and electrical mismatches between cells depending on the panel curvature. We will examine such issues in future work.

TABLE I
PANEL COMPONENT MASSES AND PROPOSED CHANGES

Component	Mass (kg)
3.2mm glass	13.22
Aluminum Frame	2.62
Add brace (example)	+0.70
Re-optimize frame (example)	-0.50
Reduce glass 0.2mm	-0.83
Double front EVA thickness	+0.68

V. Building Compressive Stress Into The Laminate

An alternative approach to placing the cells into compressive stress is to the change the materials, equipment, and recipes used during the lamination process step (LIPS approach). An example of such an approach has been previously implemented by TenKsolar where they used a backsheet containing a layer of aluminum so that during the cooling stage of lamination, the aluminum contracted more than the silicon and glass [9]. While this approach makes sense, we know of no published data documenting the comparative benefits on panel durability metrics. Here, we have explored an alternative approach involving the bending of the laminate sandwich within the laminator and during the cooldown stage immediate following lamination.

If a laminate sandwich is forced against a curved laminator insert in the early stages of lamination, the side of the cells on the inside of the curve will be in more compression and the opposite side will be in tension, averaging out to a stress state of zero. As is shown below in Fig. 9, if the laminate is pressed against a similar curved surface during a later cooldown step, the layers will all lock in together after the encapsulant crosslinks and hardens. Later when the pressure is released, the glass will largely flatten out, and since the cells are far from the neutral stress plane, this will place the cells under a larger state of "protective" compressive stress.

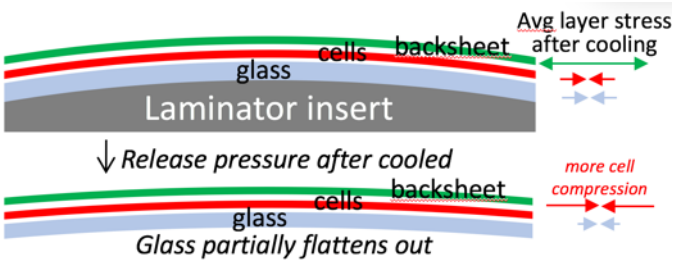

Fig. 9. Cell stress state averaged across its thickness after being laminated and cooled in a curved state as well as after pressure is released and the glass is allowed to return to a near flat state.

To explore this concept, we fabricated a curved Al insert with a single axis of bow for the laminator and encapsulated a single tabbed cell in a rectangular coupon where the direction of the bow was perpendicular to the axis of the busbars/wires. The encapsulation time was extended to compensate for the thermal mass of the insert. After the lamination step, the bladder pressure was released, and the laminate and insert were quickly moved to a cooling station where weights pressed on wooden spacers along the edges of the laminate to re-establish contact between the laminate and the Al insert (see Fig. 10).

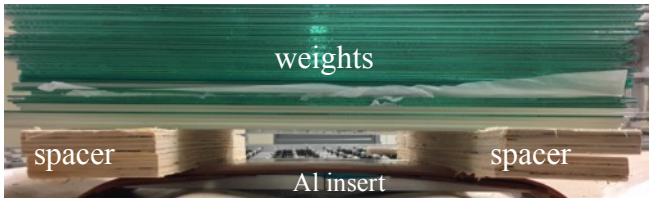

Fig. 10. Cooling the laminate in a curved state.

Three control laminates with identical construction were made in a standard manner without the curved insert, The residual bow was measured in the center 3 times on each sample by supporting the sample at the ends, placing a straight edge across the sample and using calipers as a drop gauge. Relative to bare glass, the standard samples have a slight bow toward the backsheet side due to backsheet shrinkage, while the experimental sample had a larger bow in the opposite direction, as is shown in Fig. 11a. Fig. 11b shows the fracture force for the cells as was measured in a 3-bar *Instron* mechanical load tester (see Fig. 12) where the top bar is parallel to the busbar and focuses the stress on the center busbar/wire region, and the cell was placed sunnyside up in the tester. We explored similar tests to better understand the sensitivity of fracture stress to wide range of conditions and designs in a related publication [2]. Here, the fracture force was around 50% higher for the experimental cell, suggesting that the compressive stresses have potential to reduce the tendency of cells to crack under load. Future work will explore 1) whether it is sufficient to laminate as normal and simply cool in the curved state, 2) how the results translate to full sized panels as measured by cracking vs load on the *LoadSpot* tool, and 3) whether the protective stresses are long lasting over time and after environmental chamber exposure.

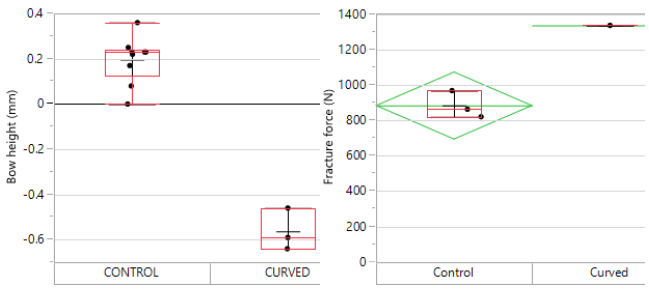

Fig. 11. a) Bow height of single cell coupons laminated and cooled as normal and in the curved state, and b) fracture force of the encapsulated cells on a 3-bar *Instron* mechanical load tester.

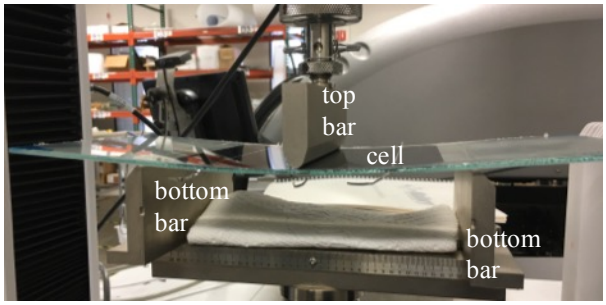

Fig. 12. Cell coupon fracture test within a 3-bar *Instron* mechanical load tester.

VI. Conclusions

We have demonstrated for the first time the effective closure of cracked solar cells and improvement in panel power by the application of rear-side pressure with the use of a brace spanning the width of the panel. Variations of such a brace could be used to strengthen new or old panels or even to heal damage in already installed and damaged panels. Future optimum panel designs in terms of durability may shift some glass mass or frame mass to one or more braces. We also demonstrated an increase in the fracture strength of cells laminated and cooled in a bent state whereby the cells are placed in state of compressive stress. Both approaches may enable an improvement in panel durability, possibly at a lower total mass and cost. Future work will involve optimization of the brace design and lamination-cooling recipes and hardware, as well as exploring the durability and cost effectiveness of such solutions. By applying either the lamination induced LIPS method or the rear loading CURL method in the factory, cell cracking during factory handling, transport, and installation may be greatly reduced, even if the protective compressive stresses are lost over time in the field.

VII. Acknowledgements

This material is based upon work supported in part by the U.S. Department of Energy's Office of Energy Efficiency and Renewable Energy, in the Solar Energy Technologies Program, under Award Number DE-EE0008152.

References

[1] A. M. Gabor, M. Ralli, S. Montminy, L. Alegria, C. Bordonaro, J. Woods, *et al.*, "Soldering induced damage to thin Si solar cells and detection of cracked cells in modules," in *21st EUPVSEC*, 2006, pp. 2042-2047.

[2] M.W. Rowell, S.G. Daroczi, D.W.J. Harwood, and A.M. Gabor, " The Effect of Encapsulant Properties and Temperature Cycling on the Fracture Strength and Performance of Encapsulated Solar Cells," in *WCPEC-7*, 2018.

[3] D.W.J. Harwood, M.W. Rowell, S.G. Daroczi, A.M. Gabor, "The Effect of Laminate Construction and Thermal History on the Fracture Strength of Solar Cells," in Poster Presentations of the 2018 Photovoltaics Reliability Workshop, Lakewood CO USA, www.nrel.gov/pv/pvmrw.html.

[4] M. Sander, S. Dietrich, et. al., "Influence of manufacturing processes and subsequent weathering on cell cracks in PV modules" in 28th EU PVSEC, 2013.

[5] A. M. Gabor, R. Janoch, A. Anselmo, J. L. Lincoln, H. Seigneur, and C. Honeker, "Mechanical load testing of solar panels - Beyond certification testing," in *IEEE 43rd Photovoltaic Specialists Conference (PVSC)*, 2016, pp. 3574-3579.

[6] E. J. Schneller, A. M. Gabor, J. L. Lincoln, R. Janoch, A. Anselmo, J. Walters, and H. Seigneur, "Evaluating Solar Cell Fracture as a Function of Module Mechanical Loading Conditions" in *IEEE 43rd Photovoltaic Specialists Conference (PVSC)*, 2017.

[7] J. Lincoln, A. M. Gabor, *et al.*" Forecasting Post-Environmental Degradation Power Loss in Solar Panels with a Predictive Crack Opening Test," in *IEEE 43rd Photovoltaic Specialists Conference (PVSC)*, 2017.

[8] C. Buerhop, S. Wirsching, A. Bemm, T. Pickel, P. Hohmann, M. Niess, C. Vodermayer, A. Huber, B. Glueck, J. Mergheim, C. Camus, J. Hauch, and C. J. Brabec, "Evolution of cell cracks in PV-modules under field and laboratory conditions," Progress in Photovoltaics: Research and Applications, vol. 26, no. 4, pp. 261-272, Dec. 2017.

[9] T. Johnson and D. Meyer, Enhanced Durability from Glass-Aluminum PV Module Package, www.nist.gov/sites/default/files/documents/el/building_materials/Enhanced-Durability-from-Glass-Aluminum-PV-module-packageten-Ksolar.pdf, last accessed 10Jun2018.